# Can we quickly flag Ultra-long Gamma-Ray Bursts?

B. Gendre, Q.T. Joyce, N.B. Orange, G. Stratta, J.L. Atteia, M. Boër

Monthly Notices
of the
ROYAL ASTRONOMICAL SOCIETY

MNRAS **486,** 2471–2476 (2019)
Advance Access publication 2019 April 13

doi:10.1093/mnras/stz1036

# Can we quickly flag ultra-long gamma-ray bursts?

B. Gendre [1,2,3★†] Q. T. Joyce,[1] N. B. Orange,[2,4] G. Stratta,[5,6] J. L. Atteia [7] and M. Boër[8]

[1] *University of the Virgin Islands, College of Science and Mathematics, 2 John Brewers Bay, 00802 St Thomas, VI, USA*
[2] *Etelman Observatory, 00802 St Thomas, VI, USA*
[3] *OzGrav-UWA, University of Western Australia, School of Physics, M013, 35 Stirling Highway, Crawley, WA 6009, Australia*
[4] *OrangeWave Innovative Science, LLC, Moncks Corner, SC 29461, USA*
[5] *INAF-Osservatorio di astrofisica e scienza dello spazio, via P. Gobetti 93/3, I-40129, Bologna, Italy*
[6] *INFN, Sezione di Firenze, I-50019 Sesto Fiorentino, Firenze, Italy*
[7] *IRAP, Université de Toulouse, CNRS, CNES, UPS, 14 Avenue Edouard Belin, F-31400 Toulouse, France*
[8] *ARTEMIS UMR 7250 UCA CNRS OCA, boulevard de l'Observatoire, CS 34229, F-06304 Nice Cedex 04, France*

Accepted 2019 March 29. Received 2019 March 26; in original form 2018 November 8

## ABSTRACT

Ultra-long gamma-ray bursts are a class of high-energy transients lasting several hours. Their exact nature is still elusive, and several models have been proposed to explain them. Because of the limited coverage of wide-field gamma-ray detectors, the study of their prompt phase with sensitive narrow-field X-ray instruments could help in understanding the origin of ultra-long GRBs. However, the observers face a true problem in rapidly activating follow-up observations, due to the challenging identification of an ultra-long GRB before the end of the prompt phase. We present here a comparison of the prompt properties available after a few tens of minutes of a sample of ultra-long GRBs and normal long GRBs, looking for prior indicators of the long duration. We find that there is no such clear prior indicator of the duration of the burst. We also found that statistically, a burst lasting at least 10 and 20 minutes has respectively 28 per cent and 50 per cent probability to be an ultralong event. These findings point towards a common central engine for normal long and ultra-long GRBs, with the collapsar model privileged.

**Key words:** methods: observational – gamma-ray burst: general.

## 1 INTRODUCTION

From an etymological point of view, gamma-ray bursts (GRBs) are observationally defined events: they are bursts of $\gamma$-ray photons. The phenomenon was discovered in the late 1960s by the Vela satellites (Klebesadel, Strong & Olson 1973), and since then has been studied with passion by generations of high-energy astronomers with various instruments dedicated to GRB research (e.g. KONUS, PHEBUS, BATSE, *BeppoSAX*, HETE-2, *Swift*; Mazets et al. 1981; Barat et al. 1992; Fishman et al. 1994; Piro et al. 1998; Ricker et al. 2003; Gehrels et al. 2004). We now know that in fact GRBs encompass different kinds of physical events. It is understood that GRBs (see Meszaros 2006, for a review) are fantastic explosions at cosmological distances due to either the merging of two compact objects (Eichler et al. 1989) or the death of supermassive stars (Woosley 1993). Soft gamma-ray repeaters (Mazets et al. 1982), or tidal disruption events (such as *Swift* J164449.3+573451; Burrows et al. 2011), are also visible in gamma-rays and could be wrongly mistaken for GRBs.

A few years ago, a new ultra-long class of GRBs has been identified (Gendre et al. 2013), and several authors have proposed various bursts to be classified as such events (e.g. Levan et al. 2014; Cucchiara et al. 2015; Lien et al. 2016). The ultra-long GRB class is still mysterious, and at the moment they are only classifiable via observational properties (see for instance Levan 2015; Ioka, Hotokezaka & Piran 2016). These events can be explained with three main classes of progenitors: an ultra-massive stellar progenitor, very similar to Pop III stars (Suwa & Ioka 2011; Nagakura, Suwa & Ioka 2012; Macpherson, Coward & Zadnik 2013); the tidal disruption of a dwarf star (MacLeod et al. 2014); and a newborn magnetar (Greiner et al. 2015).

Disentangling among the progenitor models of ultra-long GRBs is difficult, as by construction they predict the same kind and level of emission (see the interesting discussion in Ioka et al. 2016, for instance). To overcome such limitations, we are lacking key observations that could narrow the proposed models. Stratta et al. (2013) have already shown that the afterglow of ultra-long GRB 111209A is not different from any long burst one. Albeit of different types, ultra-long GRBs and normal long GRBs are

★ E-mail: bruce.gendre@uwa.edu.au
† Present address: University of Western Australia.

associated with supernovae (Greiner et al. 2015). The key to solving the nature of ultra-long GRBs, if it exists, likely resides in prompt phase multiwavelength observations. Most ultra-long GRBs last for a couple of hours (see Boër, Gendre & Stratta 2015). Though observing a phenomenon that lasts so long would seem relatively simple in this era of large-scale facilities, such data remain elusive because observational prior indicators that foreshadow these bursts are non-existent: most of these facilities being oversubscribed, each observational minute is extremely valuable, and obtaining unanticipated short-term observations (in less than 5 h) is highly competitive. A predictive method is thus necessary for observers to assess the probability that a given long GRB is in fact an ulGRB in order to perform radio, optical, or X-ray follow-up as early as possible during the prompt phase. We have studied the information available at the time of the trigger to see if such a method could be defined or if it was impossible. The purpose of this article is to report our findings.

We present in Section 2 the samples used for this study, which are classified as a gold sample, made up of genuine ultra-long GRBs (ulGRBs hereafter); a silver sample, composed of doubtful events; and a control sample of long GRBs. We then explore their spectral (Section 3) and temporal (Section 4) properties, which are discussed in Section 5 before our conclusions. In the remainder of our manuscript, all measurement errors are given at the 90 per cent confidence level, while statistical results are at the $3\sigma$ level. A flat $\Lambda$CDM (lambda cold dark matter) cosmological model ($H_0 = 72$, $\Lambda = 0.73$) is used when needed.

## 2 SAMPLE SELECTION

For this study, we focus on *Swift* data to build an homogeneous sample to avoid selection biases between different detectors. Observations available up to 2017 November were used to build our gold, silver, and control samples, based on event durations (see below).

As discussed in Zhang et al. (2014) and Boër et al. (2015), the separation between ulGRBs and long GRBs is not well defined, and various authors are using an ad hoc separation value, complicating the comparison of the samples. Lien et al. (2016), for instance, use emission lasting more than 1000 s in the 15–350 keV energy range. Boër et al. (2015) used also a duration of 1000 s but in the 0.2–10 keV band. Thus, the construction of our ulGRB (gold) and long GRB (control) samples was done carefully in order to avoid the 'grey area' where both bursts could be present. We used this grey area to build a (silver) sample of events that could or could not be ulGRBs, as a blind sample for classification tests.

We measured event duration using the method of Boër et al. (2015), which defines the prompt emission end point as the start of the steep decay phase ($T_x$), and thus the total duration of the event. While this is not the standard way (i.e. opposed to the usual $T_{90}$ measurement in $\gamma$-ray), it allows the samples to be unbiased toward the limited sensitivity of the BAT instrument in some cases.

As noted above, Boër et al. (2015) used the limit of $T_x = 10^3$s to discriminate long and ultra-long events. However, that value is not above the $3\sigma$ level of the distribution of long GRBs, and as such some these events could still be present. We considered $T_x = 10^3$ s to be the lower limit of our silver sample. The value $T_x = 5 \times 10^3$ s (where the $3\sigma$ limit is reached) was used to set the boundary between our silver and gold samples. For our control sample, we defined it as GRBs with a $T_{90}$ duration of at least 500s not belonging to any of the previous two groups to ensure that trivial bursts (i.e. those lasting a few seconds) are not used to test for ultra-long durations.

**Table 1.** The gold sample of ulGRBs with $T_x > 5 \times 10^3$ s. We list selected properties.

| Name | Duration ($T_{90}$, s) | Duration ($T_X$, s) | Redshift |
|---|---|---|---|
| GRB 101225A | >7000 | 5296 | 0.847 |
| GRB 111209A | 25 000 | 25 400 | 0.677 |
| GRB 121027A | >6000 | 8000 | 1.77 |
| GRB 130925A | 4500 | 10 000 | 0.35 |
| GRB 170714A | 420 | 16 600 | 0.793 |

**Table 2.** The silver sample of possible ulGRBs, selected with $5 \times 10^3$ s > $T_x > 10^3$ s. We list selected properties.

| Name | Duration ($T_{90}$, s) | Duration ($T_X$, s) | Redshift |
|---|---|---|---|
| GRB 060111A | 13.2 | 3243 | 5.5 |
| GRB 060218A | 2100 | 2917 | 0.03 |
| GRB 121211A | 182 | 1415 | 1.023 |
| GRB 141031A | 920 | 1100 | – |
| GRB 141121A | 1410 | <5000[a] | 1.47 |
| GRB 140413A | 140 | 3899 | – |
| GRB 161129A | 35.5 | 2000 | 0.645 |

*Note*. [a]The start of the fast X-ray decay is missing in the XRT data due to a gap in the observation. We can set only an upper limit.

**Table 3.** The control sample of long GRBs selected with $10^3$ s > $T_x > 500$ s. We list selected properties.

| Name | Duration ($T_{90}$, s) | Duration ($T_X$, s) | Redshift |
|---|---|---|---|
| GRB 081028A | 260 | 529 | 3.038 |
| GRB 090417B | 260 | 535 | 0.35 |
| GRB 111016A | 550 | 900 | 6.4 |
| GRB 111123A | 290 | 647 | 3.15 |
| GRB 111215A | 796 | 990 | 2.06 |
| GRB 121217A | 778 | 720 | 3.1 |
| GRB 130606A | 276 | 729 | 5.91 |
| GRB 140114A | 140 | 578 | 3.0 |
| GRB 150616A | 600 | 618 | – |

These criteria were used to construct the gold, silver, and control samples presented in Tables 1, 2, and 3, respectively.

It can already be observed that our gold bursts are all located at small redshifts, when compared to the other samples. Gendre et al. (2013) discussed this fact, and explained it as a selection effect due to the *Swift* trigger conditions: for more distant events the satellite would rather trigger only on the peak of the emission, thus reducing the recorded $T_{90}$. In addition, other classes of GRBs are also a very low redshift while not being ultra-long ones (e.g. Dereli et al. 2017).

One may argue that due to the time dilation, the control sample may be biased toward distant events. From Table 3, we can see that the redshifts of those bursts range from 0.35 to 6.4, and that most of the events are located close to the mean redshift value of 2.8 reported by Jakobsson et al. (2006) for normal long GRBs. We thus assume that sample not to be biased against high distance. Also, as reported in the Introduction section, we are looking for a way to classify ulGRBs within minutes, while the redshift measurement requires hours: we are not supposed to have access to this information for our study.

**Table 4.** Spectral properties of our various samples. For the gold and silver samples, we extracted the spectra during the first 300s. For the control sample, we extracted two spectra when possible: one during the first 300s, and a second one for the whole duration of the event. We report both results with the integration time in the table.

| burst | Extraction start UTC time (s) | Integration time (s) | Spectral index | Flux ($10^{-9}$ erg cm$^{-2}$ s$^{-1}$) | Reduced $\chi^2$ | d.o.f. | sample |
|---|---|---|---|---|---|---|---|
| GRB 101225A | 18:34:53 | 300 | 2.0 ± 0.7 | 1.4 ± 0.4 | 0.80 | 59 | Gold |
| GRB 111209A | 07:12:16 | 300 | 1.49 ± 0.04 | 45.7 ± 2.9 | 0.84 | 59 | Gold |
| GRB 121027A | 07:32:40 | 300 | 1.9 ± 0.2 | 6.0 ± 0.5 | 0.74 | 59 | Gold |
| GRB 130925A | 04:11:36 | 300 | 2.18 ± 0.05 | 59.7 ± 5.2 | 0.71 | 59 | Gold |
| GRB 170714A | 12:25:52 | 300 | 1.8 ± 0.3 | $5^{+9}_{-3}$ | 1.36 | 56 | Gold |
| GRB 060111A | 04:23:07 | 300 | 1.6 ± 0.2 | 4.9 ± 0.4 | 0.66 | 59 | Silver |
| GRB 060218A | 03:34:32 | 300 | 2.2 ± 0.2 | 4.8 ± 0.5 | 0.91 | 59 | Silver |
| GRB 121211A | 13:47:13 | 300 | 2.4 ± 0.4 | 3.4 ± 0.5 | 0.96 | 59 | Silver |
| GRB 140413A | 00:09:52 | 300 | 1.5 ± 0.1 | 35.5 ± 3.0 | 0.74 | 56 | Silver |
| GRB 141031A | 07:18:39 | 300 | 1.2 ± 0.4 | 3.2 ± 0.6 | 0.80 | 59 | Silver |
| GRB 141121A | 03:50:56 | 300 | 1.8 ± 0.2 | 11.2 ± 1.0 | 0.99 | 59 | Silver |
| GRB 161129A | 07:11:57 | 300 | 1.5 ± 0.1 | 10.8 ± 0.4 | 1.53 | 56 | Silver |
| GRB 081028A | 00:25:04 | 260 | 1.87 ± 0.08 | 12.8 ± 0.9 | 0.86 | 59 | Control |
| GRB 090417B | 15:20:08 | 260 | 2.2 ± 0.4 | 2.6 ± 0.4 | 0.99 | 59 | Control |
| GRB 111016A | 18:37:12 | 300 | 1.8 ± 0.2 | 10.5 ± 0.8 | 0.72 | 59 | Control |
| | | 550 | 1.9 ± 0.1 | 6.4 ± 0.5 | 0.78 | 59 | Control |
| GRB 111123A | 18:13:29 | 300 | 1.69 ± 0.06 | 20.9 ± 1.5 | 0.52 | 59 | Control |
| | | 290 | 1.68 ± 0.06 | 21.5 ± 1.6 | 0.51 | 59 | Control |
| GRB 111215A | 14:04:16 | 300 | 1.8 ± 0.3 | 6.7 ± 0.9 | 0.88 | 59 | Control |
| | | 796 | 1.6 ± 0.2 | 4.1 ± 0.5 | 1.30 | 59 | Control |
| GRB 121217A | 07:17:58 | 300 | 1.5 ± 0.2 | 4.7 ± 0.4 | 0.97 | 59 | Control |
| | | 778 | 1.61 ± 0.09 | 7.0 ± 0.5 | 0.79 | 59 | Control |
| GRB 130606A | 21:04:50 | 277 | 1.6 ± 0.1 | 8.6 ± 0.7 | 1.16 | 59 | Control |
| GRB 140114A | 11:57:52 | 140 | 2.1 ± 0.1 | 17.1 ± 1.2 | 0.90 | 59 | Control |
| GRB 150616A | 22:49:33 | 300 | 1.69 ± 0.06 | 47.4 ± 2.7 | 0.78 | 59 | Control |
| | | 600 | 1.72 ± 0.06 | 27.1 ± 1.6 | 1.08 | 59 | Control |

## 3 SPECTRAL PROPERTIES

### 3.1 Prompt spectrum

We retrieved from the *Swift* BAT archive all the prompt data related to our three samples, and performed a spectral fitting. In order to have a coherent sample, each data set has been reprocessed by the task *batbinevent* to create the spectrum. We used the version 6.22 of the FTOOLS with the latest version of the *Swift* calibration database. As we were looking for differences in the first minutes of the events, their spectrum during the first 300 s of the prompt phase was extracted. For normal long events, we also extracted the whole spectrum to decipher if differences between the first part of the event and the whole burst existed. Note that several events are lasting in the BAT band less than 300 s, while still fulfilling our filtering criteria in the XRT band.

As one can expect due to the narrow spectral band of the BAT instrument, complex models such as the Band model (Band et al. 1993) do not provide well-constrained fits. So, we concentrated on an estimation of the hardness, using a single power-law model. The results are listed in Table 4. The poor fit of GRB 170714A seems to be due to a larger background as compared to the other events. Indeed, a visual inspection of the residuals showed some random variability in the spectrum. All the other bursts are well fit by the single power-law model.

We plot in Fig. 1 the spectral index as a function of the mean flux during the first 300 s. One can clearly see a standard effect of the brightness, i.e. that faint prompt phases have a low flux and large error bars. A statistical test that accounts for the size of the error bars and the small number of events indicated that the gold and control samples are statistically similar. We did not find any discrepancies within the flux distributions of the three samples.

### 3.2 Integrated energy

Ultra-long GRBs have larger energetic budgets, so one could ask if such is built differently than for normal long events? In Fig. 2, we present the fluence of our bursts versus time. As can be seen therein, no clear pattern emerges. Ultra-long GRBs (gold sample) have similar energy emission rates as compared to normal long GRBs. One can note that one of the burst fluence plotted in this figure seems to decrease, which is not physical. This effect is due to the fact that we have used for our study only the information available *at the moment of the trigger*. For that event, the final background signal was found to be lower than the initial one: this non-physical behaviour is only due to a poor background correction.

The first derivative of the fluence (i.e. its growth rate) as a function of time provides a similar view as above, with no clear distinction between between long and ultra-long bursts. We, thus, conclude that the energy emission method is the same in these events.

## 4 TEMPORAL PROPERTIES

Lastly, the light curves of ulGRBs were investigated for patterns atypical to those of normal long GRBs. We found no evidence to support such, using either an FFT transformation or direct visual inspection. In the standard model view, this is perfectly plausible,

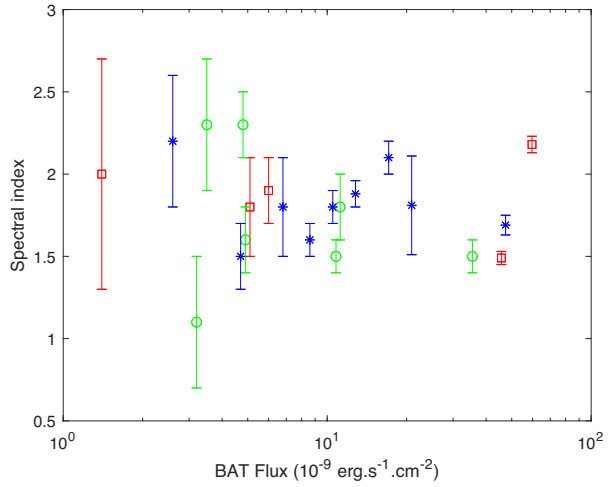


**Figure 1.** Spectral index as a function of the initial flux of the burst. We present the gold sample in red, the silver sample in black, and the control sample in blue. The flux has been extracted for the first 300 s of the burst only and is expressed in the 15–150.0 keV band.

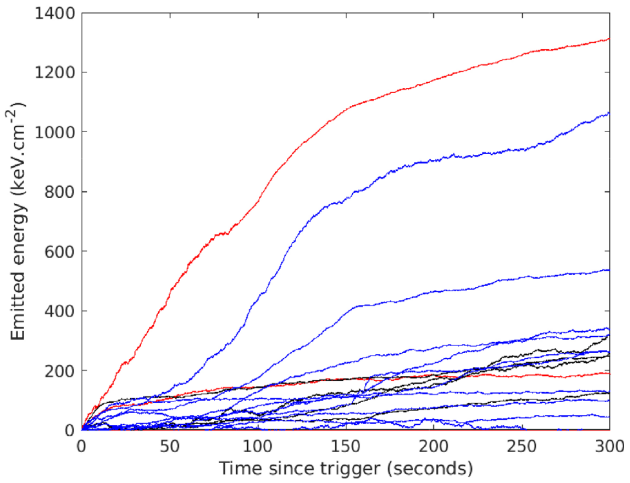


**Figure 2.** Fluence of the bursts as a function of time. The colors are the same as in Fig. 1. The fluence has been extracted for the first 300 s of the burst only and is expressed in the 15–150.0 keV band. Note that we are using the *Swift* trigger time when available, and thus some ultra-long events are quiescent during the temporal window used.

as the prompt phase temporal profile is due to internal shocks not linked to the nature of the progenitor.

We also considered the distribution of burst durations. As already noted, ulGRBs have by definition durations of at least 1000 s, and can be classified with surety once 5000 s have elapsed without seeing a steep decline in their X-ray light curves. It is thereby possible to compute a probability that a burst is an ultra-long event using the information that a burst is still in its prompt phase. Indeed, the probability that a burst lasts more than $X$ seconds knowing that it is active since $Y$ seconds increases with the value of $Y$. We set $X$ to be 5000 s, and tested various values of Y using the duration ($T_x$) distribution. These probabilities are listed in Table 5.

As observed in Table 5, if a burst lasts at least ∼20 min (1200s), then the probability that it is an ulGRB is 50 per cent. For consistency, we included the case $X = Y = 5000$ s, which obviously produces a probability of 1.0. We also note that these probabilities are likely underestimated, because X should be fixed by the number of ulGRBs in our silver sample and not arbitrarily. However, as no unique indicator was found that could sufficiently classify ulGRBs within our silver sample, it is impossible to better constrain the value of $X$.

**Table 5.** Probability that a burst is an ulGRB as a function of the minimal observed emission duration. If the emission of the burst last at least this value, then the burst could be classified as an ulGRB (assuming the emission will continue) with the associated probability.

| Duration ($T_X$, s) | Probability | Duration ($T_X$, s) | Probability |
|---|---|---|---|
| 200 | 0.0633 | 1200 | 0.4545 |
| 400 | 0.1389 | 2400 | 0.5556 |
| 600 | 0.2778 | 3600 | 0.8333 |
| 1000 | 0.4167 | 5000 | 1.0 |

## 5 DISCUSSION AND CONCLUSIONS

### 5.1 Can we define a burst to be ultra-long without the knowledge of the duration?

Boër et al. (2015) already demonstrated that long and ultra-long GRBs were different, based on their duration distribution. The boundary between these two classes is however still not sure. Gendre et al. (2013) proposed to use $10^4$ s as a cut-off limit, while Boër et al. (2015) suggested $10^3$ s. We defined this limit as $5 \times 10^3$ s, given that it resulted in a pure sample of ulGRBs, and because a significantly large sample of normal long GRBs with the presence of a few miss-identified ulGRBs would have no consequences on statistical studies.

From the first few minutes of the long and ultra-long GRBs studied here, none of the spectral or temporal properties tested were conclusive for discriminating these two burst classes. In fact, as it is clearly seen in Fig. 1, it is impossible to assess if the bursts in our silver sample are either ultra-long or normal long events. Thereby, it seems that there is no *a priori* parameter allowing the classification of ulGRBs before the end of their prompt phase.

*Swift*-BAT is clearly a limited instrument for a study such as ours, because its response bandwidth in the gamma-ray band is not very wide. We recognize that it is plausible that the/a 'correct' measurement for early phase ulGRB classification may have been overlooked by this work. For instance, Piro et al. (2014) found a blackbody component in the X-ray spectrum of GRB 130925A, and a re-analysis of GRB 111219A by Gendre et al. (2013) revealed an extra component in its *XMM–Newton* spectra, initially classified as non-thermal, that was in fact more plausibly a thermal component. Such components were also found in the observations of GRB 170714A (Piro et al., in preparation). However, this component was too faint to be detected by *Swift*-XRT, and we are limited to the observable data tested in this paper.

Clearly, even a couple of prompt phase ulGRB observations from large facilities would significantly help in understanding if an empirical indicator exists for their early classification. The probabilities listed in Table 5 show that if an event is still active after ∼20 min, there is 50 per cent of chance it will still be active for at least 2–3 h. Such information can be easily obtained by the *Swift* team and disseminated as an automated GCN, flagging them as potential ultra-long events (it should be noted that any event with

an activity of ∼20 min is already inside our silver sample), to allow for a deep and fast follow-up.

### 5.2 What are the consequences for the standard model?

Our findings are important for the study of the central engine and progenitor of ulGRBs. Ioka et al. (2016) have indicated that none of the models can be totally ruled out by the current observations. So it is possible that the progenitors of long and ultra-long GRBs are intrinsically different. However, both in the prompt phase (this work) and in the afterglow phase (Stratta et al. 2013), long and ultra-long events are extremely similar. Other studies (e.g. atteia et al. 2017), focusing on standard properties, have also found that normal long GRBs and ulGRBs were behaving similarly. This clearly indicates that the central engines, albeit being active longer for ulGRBs, have the same properties in both cases and may be similar.

A consequence of similar long and ultra-long GRB central engines is obvious: the various progenitor models have to produce the same 'class' of central engines. If one considers the magnetar model (Usov 1992) for the central engine of long GRBs, then obviously it is also favored for ulGRBs. However, in such a case, the criticisms formulated in Ioka et al. (2016) and Gendre et al. (2013) against this model (mostly the energy budget) still hold.

The white dwarf tidal disruption events defended by Ioka et al. (2016) may also be plausible in the case of very close encounters, albeit their model uses a black hole of $10^5$ $M_\odot$. However, one would then need to explain how to produce normal long GRBs with such a central engine, compatible with the various and numerous supernovae-associations reported in the literature (e.g. Kawabata et al. 2003; Stanek et al. 2003). Because this progenitor is a known emitter of gravitational waves (GWs) in the band of *LISA* (Anninos et al. 2018), GW observations could play a key role to validate this hypothesis.

Lastly, if one considers the collapsar model (Woosley 1993) for long GRBs, we are dealing with a stellar mass black hole as the central engine, accreting the remains of the star. Our findings would favour this hypothesis. In particular, given that the difference in duration would only be due to the difference in size of the stars, as already argued in Gendre et al. (2013).

### 5.3 Possible bias on our analysis

As indicated in the Introduction section, several models could explain ulGRBs. For instance, if long GRBs are a result of the collapsar model of Woosley (1993), while ulGRBs are due to the white dwarf tidal disruption model of MacLeod et al. (2014), a difference in the temporal and spectral regimes of long GRBs versus ulGRBs would be expected. That is, the collaspar model is based on chaotic emission of matter inside a jet, and emission from a white dwarf disruption is linked to an accretion disc. As we found no evidence of different observational characteristics to suggest the same global model, speculations on various models that could explain either of these types of GRBs were deferred to this section.

As we stated earlier, long GRB and ulGRB populations reside at different distances from the Earth. Thus, one could question if redshift effects mask observational differences between these two populations. The effects of redshifts on observations relate to time dilation, peak energy position, and the flux observed in a fixed band in the observer frame. The first two of these imply a factor of $(1 + z)^{-1}$ in the temporal range and $(1 + z)$ in the spectral range. If we consider mean values, reshift effects indicate that a factor $\Delta = (1 + 1)/(1 + 3) = 0.5$ exists between two populations. In the temporal domain, no power diagram shifts were found that would be interpreted as evidence to favour such effects. On spectral aspects, redshift effects should divide in half the peak energy value ($E_p$), and lead to the appearance of a harder spectral slope of ulGRBs relative to long GRBs, if all the intrinsic values of $E_p$ for long GRBs were in the 80–100 keV range. We rule out this hypothesis by pointing out that the statistical studies of Fermi (Yu et al. 2016) or Amati (2006) showed that $E_p$ peaks at larger values with a very broad distribution.

The redshift effect on observed fluxes would be apparent in Fig. 2, as a decreasing growth rate of the blue curves, compared to the red ones. It is beyond this study to suggest an estimate of how this effect would change the results of this figure. We speculate that a study based on the rest-frame properties, however, could shed more light on the similar and/or differing central engine properties of long GRBs and ulGRBs. From this work, a naive estimate based solely on the distance would be inaccurate as the *detection bandwidth* is also affected by redshifts, and the *k*-correction needed for clarifying it is highly model dependent. In addition, obviously the selection biases of ulGRB selection we discussed in the Introduction section would also require correction, as there would be a whole fraction of distant ulGRBs not present on Fig. 2 then. Particularly, if one considers that Pop III stars would lead to ulGRBs (Suwa & Ioka 2011; Nagakura et al. 2012; MacPherson et al. 2013). Again, these would be hard to locate on our Fig. 2, as we don't precisely know their properties: the fact they were not detected may not *only* be related to their brightness but *also* the triggering algorithm of the detecting instrument being less sensitive to their spectral or temporal properties (Gendre et al. 2013), or to a redshift so large that the BAT band would be located above a few MeV in the rest frame. The only conclusion we can reach here is that some events have similar redshifts (GRB 130925A and GRB 090417B, for instance), and similar properties in each of our tests, while belonging to two diverse groups. As no correction could change this result, we are confident that our work, even if affected by redshift differences, provides a good representation of the true initial distributions.

### 5.4 The future of the science of ulGRBs

In this paper, we concentrated on possible markers available near the *Swift* trigger time to classify GRBs as ultra-long types. Other tests are possible, and could lead to new questions. For instance, a simple comparison of the BAT duration and the $T_X$ measurement (similar to a duration in the X-ray band) clearly indicates that ulGRBs should be soft events, and one could ask if these events are not in fact ulXRFs. However, the access of the hardness ratio is currently only available a few hours after the trigger. *Swift* is thus not the best suited observatory to answer these kinds of questions. However, in the future we may have more success in addressing such with new instruments in preparation.

*SVOM* (Wei et al. 2016; Gonzalez & Yu 2018), to be launched in a couple of years, is well suited for ulGRB studies. Most of all because it will observe the same direction for long periods (typically several hours), and possesses an image trigger extending to 20 min and possibly longer that will simplify efforts to detect and recognize ulGRBs (Dagoneau et al. 2018). The multiwavelength capability of *SVOM* will allow the prompt emission to be monitored simultaneously in the visible (GWAC), hard X-rays (ECLAIRs), and gamma-rays (GRM), while for the afterglow emission this will be in NIR and visible (GFTs and VT), and in X-rays (MXT) – providing detailed diagnostics to the ulGRB class of events.

In the more distant future, THESEUS (Amati et al. 2018) will provide sky surveys over a very wide energy band (0.3 keV − 20 MeV) for the detection of ulGRBs with an unprecedented large sensitivity. Such is very important for faint ulGRBs, as it will provide very good resolution of their recorded spectra and light curves (Stratta et al. 2018). The *SVOM* and THESEUS experiments may allow us to carry out tests that we were unable to perform in this study. For instance, the monitoring of the soft-to-hard X-ray hardness evolution during the prompt emission (i.e. since the beginning of the burst).

Lastly, as indicated previously, several proposed ulGRB progenitors are also GW emitters. Thereby, the next generation of GW instruments (the Einstein Telescope and possibly LISA), which will have a horizon encompassing the mean distance of ulGRBs (Punturo et al. 2010), will provide unprecedented multimessenger studies. We cannot exclude the possibility that the markers we are looking for appear more clearly in the GW signal.

## ACKNOWLEDGEMENTS

We would like to thank the anonymous referee who helped improving the text of this paper. We gratefully acknowledge support through NASA-EPSCoR grant NNX13AD28A. B.G. and N.B.O. also acknowledge financial support from NASA-MIRO grant NNX15AP95A, and NASA-RID grant NNX16AL44A. Parts of this research were conducted by the Australian Research Council Centre of Excellence for Gravitational Wave Discovery (OzGrav), through project number CE170100004. This research has been partly made under the auspices of the FIGARONet collaborative network supported by the Agence Nationale de la Recherche, program ANR-14-CE33. We thank Eric Howell and David Coward for useful discussion during the preparation of this article.

## REFERENCES

Amati L., 2006, MNRAS, 372, 233
Amati L. et al., 2018, Adv. Space Res., 62, 191
Anninos P., Fragile P. C., Olivier S. S., Hoffman R., Mishra B., Camarda K., 2018, ApJ, 865, 3
Atteia J.-L. et al., 2017, ApJ, 837, 119
Band D. et al., 1993, ApJ, 413, 281
Barat C., Dezalay J. P., Talon R., Syunyaev R., Kuznetsov A., Terekhov O., 1992, AIPC, 265, 43
Boër M., Gendre B., Stratta G., 2015, ApJ, 800, 16
Burrows D. N. et al., 2011, Nature, 476, 421
Cucchiara A. et al., 2015, ApJ, 812, 122
Dagoneau N., Schanne S., Gros A., Cordier B., SF2A-, 2018, Proceedings of the Annual meeting of the French Society of Astronomy and Astrophysics, Detection capability of Ultra-long Gamma Ray Bursts with the ECLAIRs telescope aboard the SVOM mission
Dereli H., Boër M., Gendre B., Amati L., Dichiara S., Orange N. B., 2017, ApJ, 850, 117
Eichler D., Livio M., Piran T., Schramm D. N., 1989, Nature, 340, 126
Fishman G. J. et al., 1994, ApJS, 92, 229
Gehrels N. et al., 2004, ApJ, 611, 1005
Gendre B. et al., 2013, ApJ, 766, 30
Gonzalez F., Yu S., 2018, SPIE, 10699, 1069920
Greiner J. et al., 2015, Nature, 523, 189
Ioka K., Hotokezaka K., Piran T., 2016, ApJ, 833, 110
Jakobsson P. et al., 2006, A&A, 447, 897
Kawabata K. S. et al. 2003, ApJ, 593, L19
Klebesadel R. W., Strong I. B., Olson R. A., 1973, ApJ, 182, L85
Levan A. J., 2015, J. High Energy Phys., 7, 44
Levan A. J. et al., 2014, ApJ, 781, 13
Lien A. et al., 2016, ApJ, 829, 7
MacLeod M., Goldstein J., Ramirez-Ruiz E., Guillochon J., Samsing J., 2014, ApJ, 794, 9
Macpherson D., Coward D. M., Zadnik M. G., 2013, ApJ, 779, 73
Mazets E. P., Golenetskii S. V., Gurian Iu. A., Ilinskii V. N., 1982, Ap&SS, 84, 173
Mazets E. P., , et al., 1981, Ap&SS, 80, 3
Mészáros P., 2006, Rep. Prog. Phys., 69, 2259
Nagakura H., Suwa Y., Ioka K., 2012, ApJ, 754, 85
Piro L. et al., 1998, A&A, 329, 906
Piro L. et al., 2014, ApJ, 790, L15
Punturo M. et al., 2010, CQGra, 2719, 4002
Ricker G. R. et al., 2003, AIPC, 662, 3
Stanek K. Z. et al., 2003, ApJ, 591, L17
Stratta G. et al., 2013, ApJ, 779, 66
Stratta G. et al., 2018, Adv. Space Res., 62, 662
Suwa Y., Ioka K., 2011, ApJ, 726, 107
Usov V. V., 1992, Nature, 389, 635
Wei J. et al., 2016, Proceedings of the Workshop on Report on the scientific prospect of the SVOM mission, held from 11th to 15th April, 2016 at Les Houches School of Physics, France
Woosley S. E., 1993, ApJ, 405, 273
Yu H.-F. et al., 2016, A&A, 588, A135
Zhang B.-B., Zhang B., Murase K., Connaughton V., Briggs M. S., 2014, ApJ, 787, 66

This paper has been typeset from a TEX/LATEX file prepared by the author.